

## Supplementary Materials for **Shear-wave anisotropy reveals pore fluid pressure–induced seismicity in the U.S. midcontinent**

Keith A. Nolte, George P. Tsoflias, Tandis S. Bidgoli, W. Lynn Watney

Published 13 December 2017, *Sci. Adv.* **3**, e1700443 (2017)

DOI: 10.1126/sciadv.1700443

### **This PDF file includes:**

- fig. S1. Plot of the Wellington CO<sub>2</sub> Sequestration Monitoring network (ZA) earthquake catalog consisting of 1676 events ranging in  $M$  from 0.4 to 4.3 and depth from 1 to 11 km.
- fig. S2. Depth and magnitude distributions of the 150 earthquakes used in this study.
- fig. S3. Plot of the minimization of the second eigenvalue ( $\lambda_2$ ) in  $\phi$  and  $\delta t$  space from waveforms shown in fig. S4.
- fig. S4. Plot of raw channel data from station WK15 of an  $M$  2.7 earthquake that occurred in July 2015.
- fig. S5. Hodogram plots of 0.1-s increments corresponding to the 2-s time window identified in fig. S4.
- fig. S6. Hodogram plot of  $S$ -wave splitting that aligns with the maximum horizontal stress at approximately  $75^\circ$  (marked with red dashed lines).
- Additional Acknowledgments

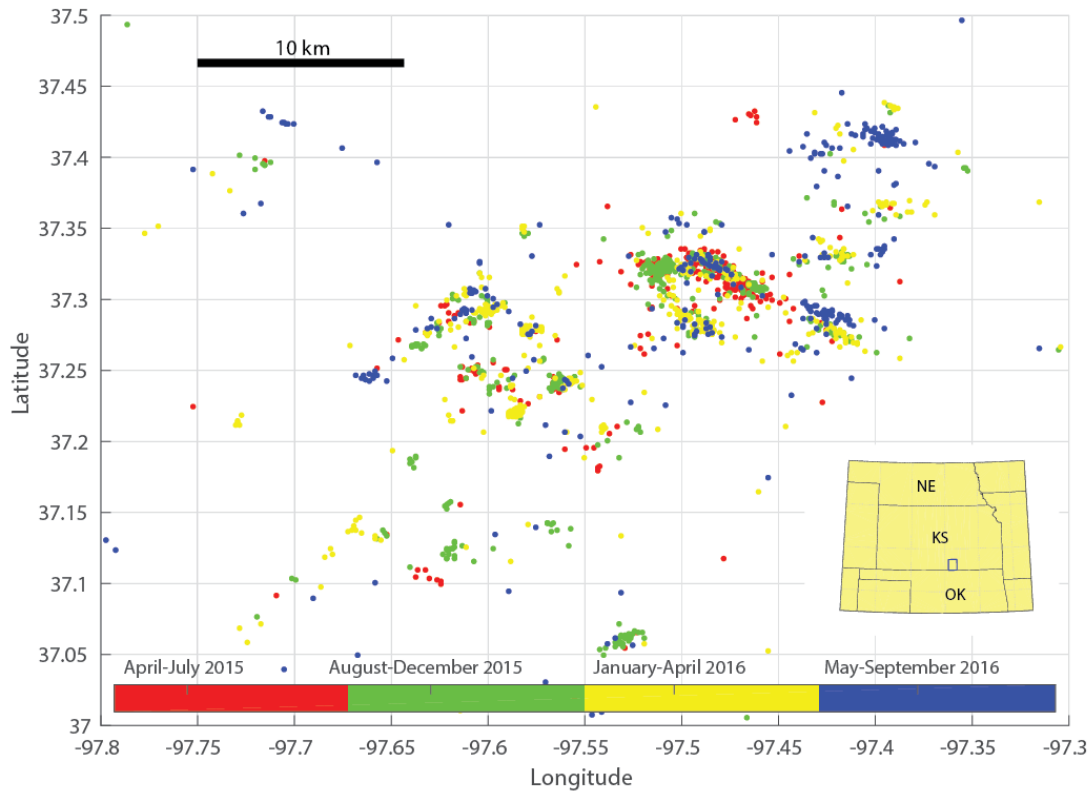


**fig. S1. Plot of the Wellington CO<sub>2</sub> Sequestration Monitoring network (ZA) earthquake catalog consisting of 1676 events ranging in  $M$  from 0.4 to 4.3 and depth from 1 to 11 km.** Earthquakes are color-coded by time of occurrence. It can be seen that the recent events (blue color) are most common in the central and northeast region of the study area, which was not active in the earlier time periods. Each color represents 150 days with a total of 161 earthquakes in red, 698 in green, 426 in yellow, and 391 in blue.

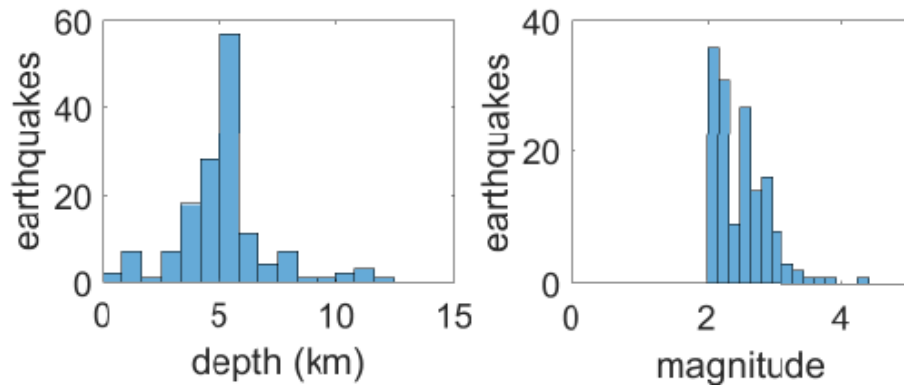


**fig. S2. Depth and magnitude distributions of the 150 earthquakes used in this study.** Most common event depth is 5 km, which is the standard reported depth for very shallow earthquakes in the USGS earthquake catalog. A low magnitude cut off of 2.0 was used in the study.

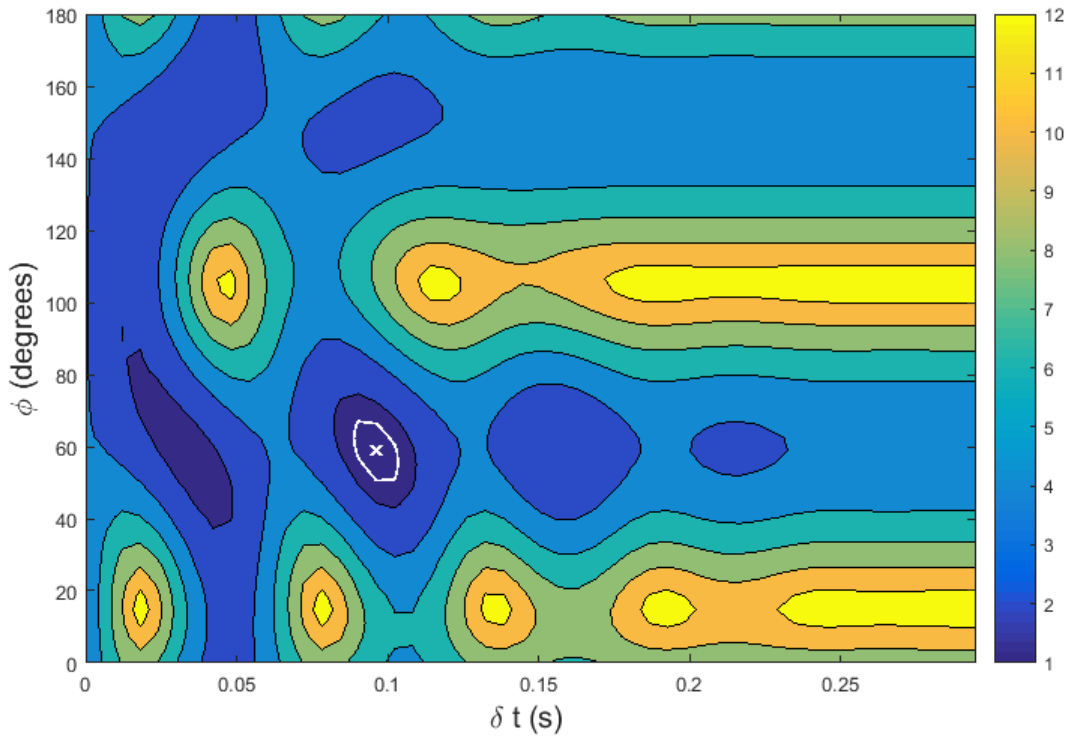


**fig. S3. Plot of the minimization of the second eigenvalue ( $\lambda_2$ ) in  $\phi$  and  $\delta t$  space from waveforms shown in fig. S4.** Minimizing  $\lambda_2$  is the chosen mathematical way to return a covariance matrix that is closest to being singular. With no noise the covariance matrix will return  $\lambda_1$  as the only non-zero eigenvalue (31). The white marker (x) is the best solution and the white contour line is an estimate of the 95% confidence interval. Angles are from  $0^\circ$  to  $180^\circ$ , where  $0^\circ$  is west and  $180^\circ$  is east. This solution of approximately  $60^\circ$  is therefore  $30^\circ$  west of north or  $330^\circ$ .

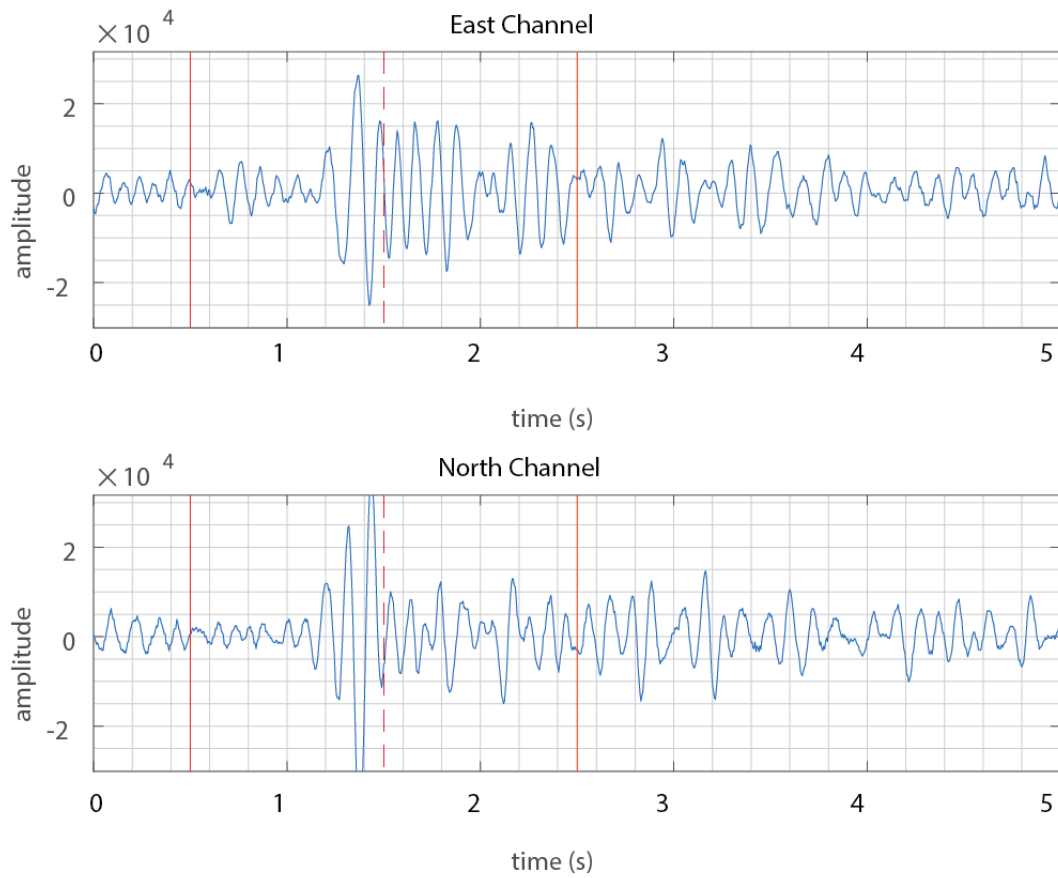


**fig. S4. Plot of raw channel data from station WK15 of an  $M$  2.7 earthquake that occurred in July 2015.** Red solid lines indicate the 2-second window seen in hodogram plots of fig. S6. Red dashed line separates the first 10 plots from the second 10 plots shown in fig. S6.

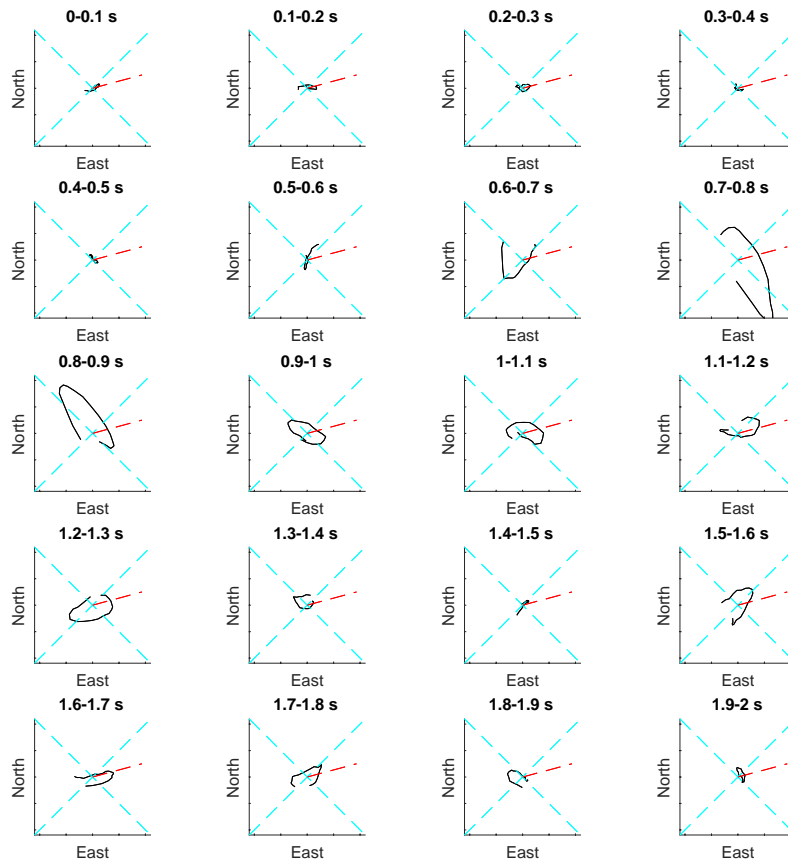


**fig. S5. Hodogram plots of 0.1-s increments corresponding to the 2-s time window identified in fig. S4.** The time stamp is shown at the top of each hodogram panel. All plots are normalized to the same axis values, making the first arrival often the largest magnitude plot. The first arrival can be seen in hodograms from 0.6 s to 0.9 s of the 2 s window. It is identified by the elliptical motion as well as the magnitude of motion. The particle elliptical motion long axis shows a  $90^\circ$  offset from the regional maximum horizontal stress orientation (approximately  $75^\circ$ ) marked by the red dashed lines. The first arrival was chosen based on time windows that exhibit the same direction of elliptical motion.

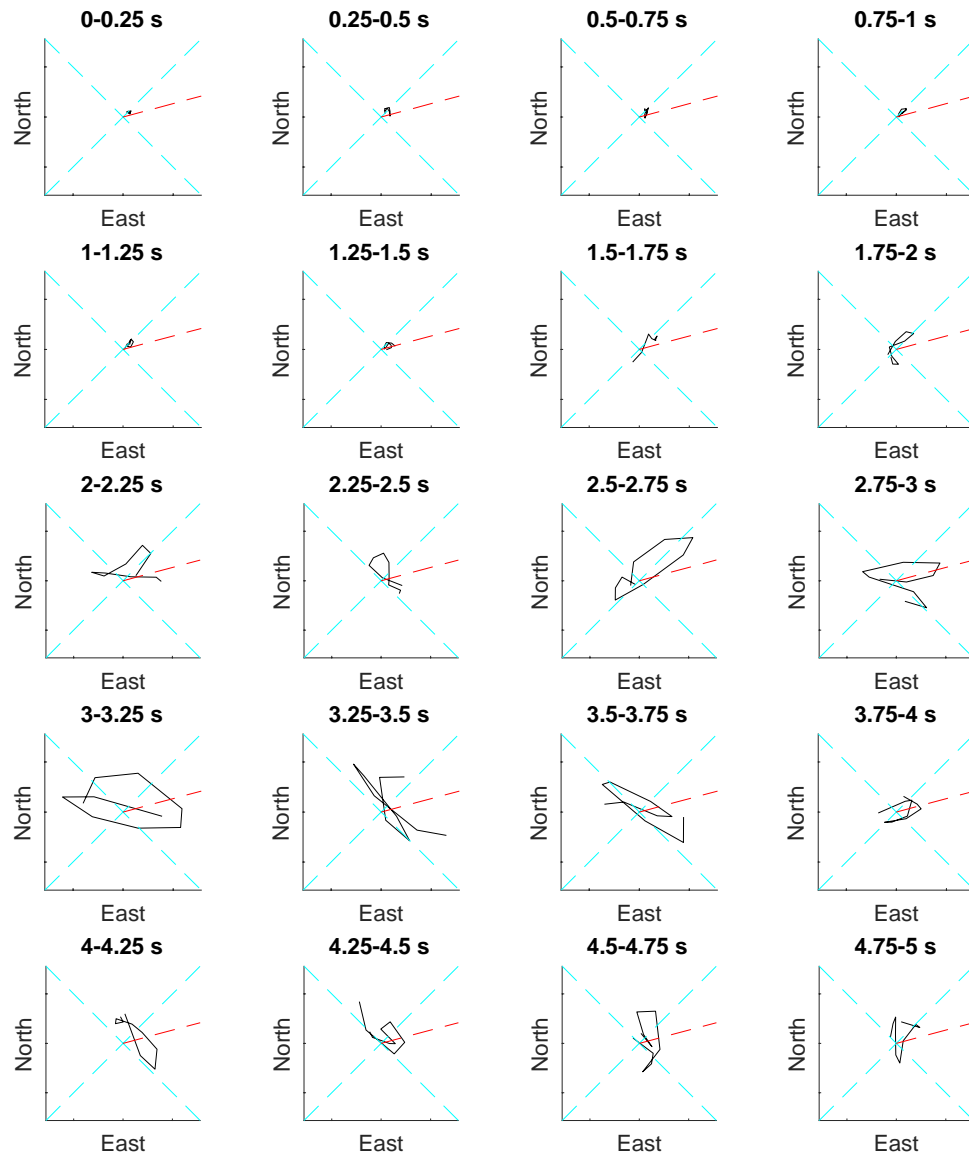


**fig. S6. Hodogram plot of S-wave splitting that aligns with the maximum horizontal stress at approximately  $75^\circ$  (marked with red dashed lines).** The first arrival can be seen from 2-3 s. This data corresponds to an  $M_w$  2.7 earthquake in February 2012. Each hodogram displays a 0.25 second increment cross-plot. Cross-plot panels have a longer duration than fig. S5 because the sampling rate of the waveforms is lower.

## **Additional Acknowledgments**

This research was supported by the U.S. Department of Energy-National Energy Technology Laboratory (DOE-NETL) under grant no. DEFE0002056. The project is managed and administered by the Kansas Geological Survey and funded by DOE/NETL and cost-sharing partners. Additional support was provided by the University of Kansas Department of Geology, and the University of Kansas Interdisciplinary Carbonates Consortium (KICC) project INS0074816.

The seismic instruments were provided by the Incorporated Research Institutions for Seismology (IRIS) through the PASSCAL Instrument Center at New Mexico Tech. Data collected will be available through the IRIS Data Management Center. The facilities of the IRIS Consortium are supported by the National Science Foundation under Cooperative Agreement EAR-1261681 and the DOE National Nuclear Security Administration. The facilities of IRIS Data Services, and specifically the IRIS Data Management Center, were used for access to waveforms, related metadata, and/or derived products used in this study. IRIS Data Services are funded through the Seismological Facilities for the Advancement of Geoscience and EarthScope (SAGE) Proposal of the National Science Foundation under Cooperative Agreement EAR-1261681. Pressure data is provided by J. Victorine (Kansas Geological Survey) and P. Simpson (Trilobite Testing). D. Wreath and Berexo provided access to the Wellington field site.

Global Seismographic Network (GSN) is a cooperative scientific facility operated jointly by the Incorporated Research Institutions for Seismology (IRIS), the United States Geological Survey (USGS), and the National Science Foundation (NSF), under Cooperative Agreement EAR-1261681. Data from the TA network were made freely

available as part of the EarthScope USArray facility, operated by Incorporated Research Institutions for Seismology (IRIS) and supported by the National Science Foundation, under Cooperative Agreements EAR-1261681. Data from the GS network are freely available from the U.S. Geological Survey Earthquake hazards Program, Geologic Hazards Science Center. <http://earthquake.usgs.gov/monitoring/anss/>

Nanometrics Seismological Instruments (2013): Nanometrics Research Network.  
International Federation of Digital Seismograph Networks. Other/Seismic Network.  
doi:10.7914/SN/NX

This report was prepared as an account of work sponsored by an agency of the United States government. The United States government, any agency thereof, or any of its employees do not make any warranty, express or implied, or assume any legal liability or responsibility for the accuracy, completeness, or usefulness of any information, apparatus, product, or process disclosed, or represent that its use would not infringe privately owned rights. Reference herein to any specific commercial product, process, or service by trade name, trademark, manufacturer, or otherwise does not necessarily constitute or imply its endorsement, recommendation, or favoring by the United States government or any agency thereof. The views and opinions of authors expressed herein do not necessarily state or reflect those of the United States government or any agency thereof.